American Mineralogist, Volume 71, pages 105–110, 1986

EPR study of Fe^{3+} centers in cristobalite and tridymite[1]

H. Rager

Fachbereich Geowissenschaften der Universität Marburg
Lahnberge, 3550 Marburg, Germany (FRG)

and H. Schneider

Forschungsinstitut der Feuerfest-Industrie
An der Elisabethkirche 27, 5300 Bonn, Germany (FRG)

Abstract

Electron paramagnetic resonance spectra were taken from powder specimens of cristobalite and tridymite at 9.16 GHz and temperatures between −120°C and 300°C. The spectra exhibit significant signals around $g_{eff} = 4$ which arise from Fe^{3+} ions in strong orthorhombic crystal fields. Fe^{3+} is assumed to substitute for Si^{4+} in both cristobalite and tridymite. The charge deficiency produced thereby is compensated by a nearest interstitially incorporated Na^+ ion. In cristobalite two crystallographically different Fe^{3+} centers occur which indicate a possible symmetry lowering of the space group symmetry of low cristobalite from $P4_12_12$ to its subgroup $C222_1$. The broadening of the electron paramagnetic resonance signals in tridymite is associated with a certain number of Fe^{3+} centers differing so slightly that their particular signals cannot be resolved.

Introduction

Many data on the microchemistry of lunar (e.g., Frondel, 1975, p. 163–182; Mason, 1972), meteoretical (e.g., Wlotzka et al., 1983), and of terrestrial tridymites and cristobalites (e.g., Mason, 1953; Smith and Steele, 1984), and of tridymites and cristobalites from refractory-grade silica bricks (e.g., Patzak and Konopicky, 1962; Schneider et al., 1980; Seifert-Kraus and Schneider, 1984) have been published in recent years. Most modern microprobe analyses have yielded impurity contents below 1.5 wt.%, with the exception of some lunar and meteoretical cristobalites and tridymites which contain foreign oxides up to 4 wt.%. Most investigators have believed that Al_2O_3, TiO_2, Na_2O, and K_2O are the main impurity compounds. Measurable amounts of iron oxide[2] have been described in tridymites and cristobalites of lunar rocks, especially in Apollo 12 samples (with FeO up to 1.96 wt.%, Busche et al., 1971). Studies on the microchemistry of tridymites and cristobalites from used silica bricks of open hearth furnaces (Schneider and Majdic, 1984) have yielded maximally 0.2 wt.% Fe_2O_3 incorporated into silica.

An interstitial entry of the large alkali and alkaline-earth ions into the relatively wide channels and voids of the tridymite and cristobalite structure can be assumed. The charge excess produced that way is compensated by substitution of Si^{4+} by Al^{3+} at tetrahedral lattice sites (e.g., Seifert-Kraus and Schneider, 1984; Smith and Steele, 1984). Though Seifert-Kraus and Schneider (1984) provided evidence for tetrahedral incorporation of Ti^{4+}, recent investigations have shown that Ti may also enter the silica structures interstitially under special circumstances. Schneider and Majdic (1984) mentioned that Fe^{3+} is incorporated into the tetrahedra at the place of Si^{4+}. They believe that charge compensation is achieved by alkali ions or by interstitially incorporated Fe^{3+}. The EPR study presented here was undertaken to provide more details on the iron-incorporation mode.

Sample material

The samples stem from a refractory silica brick which was used in the hanging roof (melting zone) of a flat glass tank for about ten years.[3] The temperature at the hot front of the brick was about 1560°C and 400°C at the cold end (see Seifert-Kraus and Schneider, 1984). The brick shows a distinct zoning perpendicular to the temperature gradient. The cristobalite sample C1 was taken from the hot side of the brick where cristobalite was the only crystalline phase coexisting with a small amount of glass (≤5 wt.%). Behind the cristobalite zone a tridymite zone developed, the boundary between both zones being rather sharp. The tridymite sample T1 was taken from the brick zone adjacent to the cristobalite-tridymite boundary, where tridymite was the only crystalline phase coexisting with some

[1] Dedicated to Prof. Dr. W. von Engelhardt on the occasion of his 75th birthday.

[2] There is no information on the degree of oxidation of iron.

[3] Literature on the composition, high-temperature behavior and technical use of refractory-grade silica bricks is reviewed by Chesters (1973).

0003–004X/86/0102–0105$02.00

Table 1. Origin and composition of samples used for EPR-analysis

Sample key	Phase content	Origin	Chemical composition (wt %) Al_2O_3	SiO_2	Fe_2O_3	TiO_2	CaO	K_2O	Na_2O	Analysis technique used
T 1	Tridymite+	Used silika bricks from the roof of a glass tank	0.20	99.5	- *	0.14	-	-	0.13	XRF/EMA
C 1	Cristobalite+		0.35	98.9	- *	0.17	-	-	0.14	XRF
C 2	Cristobalite+	Heat-treatment of sample T 1 1550°C (5 h)	see sample T 1							
G	Glass§	1730°C (2 h)	see sample T 1							

+ The glass phase coexisting with crystalline phases was washed out by H_3PO_4 treatment of the sample.

§ Homogeneous glass phase without inclusions (microscopic observation).

* Below detection limit.

XRF: X-ray fluorescence analysis.

EMA: Electron microprobe analysis.

glass (≤ 10 wt.%). A more detailed description of the silica material is given by Seifert-Kraus and Schneider (1984).

In order to make the samples glass-free the cristobalite C1 and tridymite T1 samples were treated with H_3PO_4 using a method developed for refractory silica materials.[4] Parts of the H_3PO_4-treated tridymite sample T1 were annealed in a voltage-stabilized high-temperature furnace at 1550°C (sample C2) and 1730°C (sample G) and subsequently quenched to room temperature. X-ray analyses indicated that sample C2 consisted of cristobalite and sample G of a glass phase. Microscopic observation showed that the glass phase was homogeneous and did not contain inclusions.

Experimental procedure

Chemical analysis

Bulk chemical analyses of the H_3PO_4-treated samples were performed by standard X-ray fluorescence techniques using a computer-controlled X-ray spectrometer. Microanalyses were carried out on polished sections using a microprobe with three wave length dispersive spectrometers. Weight percentages were calculated from measured net intensities with a program correcting the influence of atomic number, absorption, and fluorescence (ZAF process). The resolution of adjacent points was about 2 μm. In order to avoid a possible sodium loss by evaporation a beam diameter of 10 μm was used. All samples were X-ray examined for phase identification with standard powder goniometer techniques. Microstructure and phase content of the starting materials were determined from thin sections using a polarizing microscope.

Electron paramagnetic resonance (EPR)

The EPR measurements were performed on about 60 mg of the powdered samples. The EPR spectra were taken at X-band frequency with a Varian spectrometer using 100 kHz modulation. The temperature dependence of the spectra was studied between −120°C and 300°C. The observed EPR signals were labeled by their effective g values. g_{eff} is defined by the relation

$$h\nu = g_{eff}\beta B.$$

B is the external magnetic field at which the EPR signal appears, ν the microwave frequency used, β the Bohr magneton, and h Planck's constant. The frequency was determined by a frequency counter (HP 5340A) and the magnetic field scale was calibrated using proton nuclear magnetic resonance.

[4] A detailed description of this method will be provided on request.

Results

Chemical composition

The X-ray fluorescence (XRF) and electron microprobe analyses (EMA) of the cristobalite and tridymite samples, C1 and T1, exhibited a total impurity content below 1 wt.% with Al_2O_3, Na_2O, and TiO_2 as foreign oxides (Table 1). The EPR measurements revealed that the samples contained also some hundred ppm of iron oxide.

EPR spectra

EPR spectra taken at liquid helium temperature yielded no evidence for the occurrence of Ti^{3+} and/or Fe^{2+}. Therefore, all EPR signals observed in the cristobalite and tridymite samples are associated with Fe^{3+}.

In cristobalite a group of EPR signals is observed around $g_{eff} = 4$ with intensity which decreases with increasing temperature (Fig. 1). At −120°C the signal around $g_{eff} = 4.3$ is split into two components with $g_{eff} = 4.33$ and 4.3. Both components have similar line widths. A further broader signal appears at $g_{eff} = 4.22$. With increasing temperature these signals merge together and their common center shifts to higher g_{eff} values (lower magnetic fields). The signal at $g_{eff} = 3.92$ shows a low fine structure at

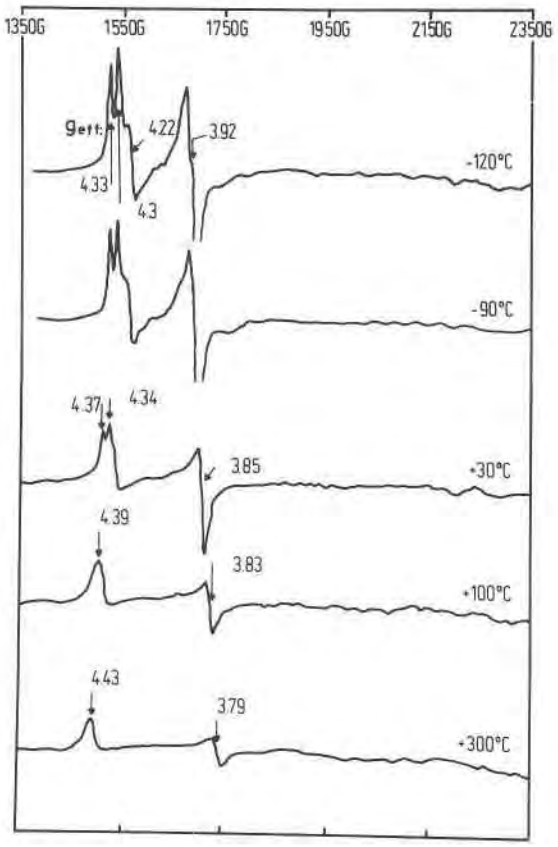

Fig. 1. EPR spectra of cristobalite at 9.16 GHz and various temperatures. The spectra were taken using a modulation amplitude of 5 G and a microwave power of 10 mW. The maximum error of g_{eff} is ±2%.

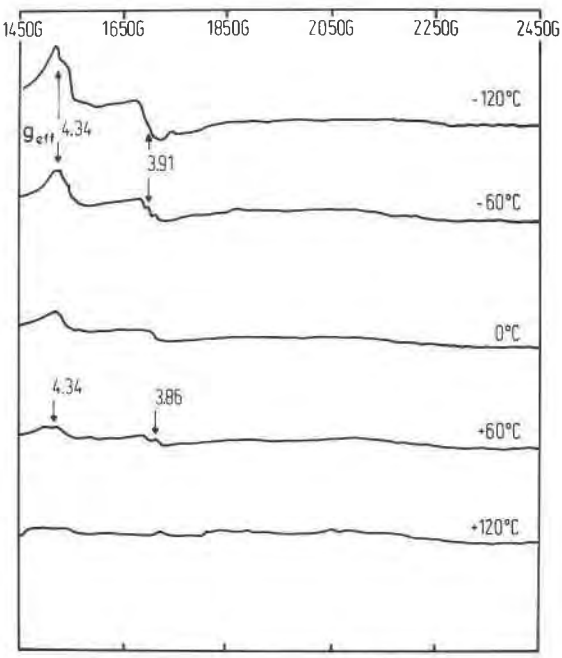

Fig. 2. EPR spectra of tridymite at 9.16 GHz and various temperatures. The spectra were taken using a modulation amplitude of 5 G and a microwave power of 10 mW. The maximum error of g_{eff} is ±2%.

−120°C which disappears at elevated temperature. Simultaneously the signal is shifted to lower g_{eff} values (higher magnetic fields).

Tridymite has a similar EPR spectrum to cristobalite with a group of EPR signals around $g_{eff} = 4$. The signal intensity decreases with increasing temperature. Contrary to the cristobalite patterns, the signal at $g_{eff} = 4.34$ shows an insignificant fine structure at −120°C which decreases with increasing temperature (Fig. 2). While the position of the signal at $g_{eff} = 4.34$ remains constant on the magnetic field scale, the signal at $g_{eff} = 3.91$ seems to shift towards lower g_{eff} values (higher magnetic fields) with increasing temperature. At 120°C all EPR signals are vanished.

The glass sample G shows one EPR signal at $g_{eff} = 4.2$ and another one at $g_{eff} = 2$. The signal intensity decreases with increasing temperature (Fig. 3). No significant shift of the EPR signals to lower or higher magnetic fields is observed with increasing temperature. A third EPR signal appears around $g_{eff} = 8$ with a line width of 1600 G or more. The intensity of this signal increases with temperature.

EPR spectra of cristobalite, tridymite and of the glass sample have also been recorded at room temperature sub-

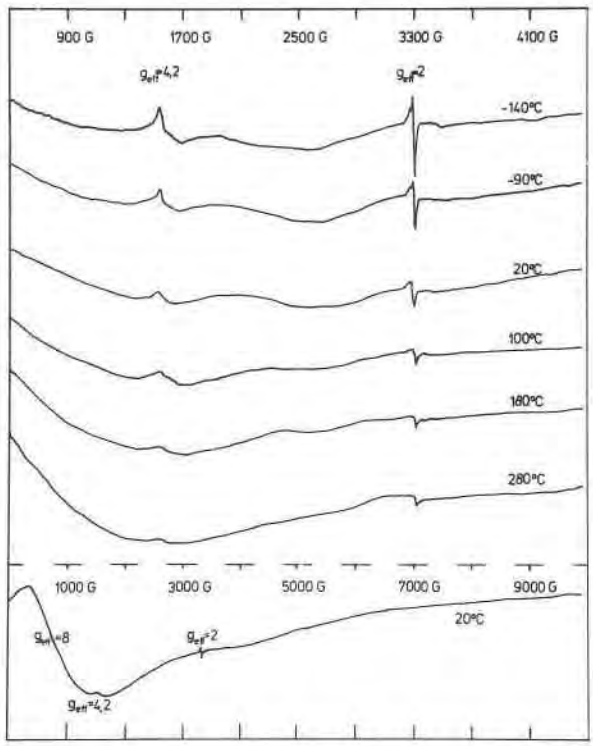

Fig. 3. EPR spectra of a glass phase at 9.16 GHz and various temperatures. The spectra were taken using a modulation amplitude of 5 G and a microwave power of 2 mW. In the lower part the range of the magnetic field is expanded to show the broad EPR signal at $g_{eff} = 8$. The maximum error of g_{eff} is ±2%.

sequent to the measurements of the temperature dependence of the spectra. No significant variation in width, position, and intensity of the EPR signals could be observed, indicating reversibility of the temperature-induced change of the spectra.

Discussion

In the high spin ground state, ^6S, Fe^{3+} ions undergo no first order spin orbit interactions and g is expected to lie near the free electron value of 2. Since experimental data reveal g_{eff} values much higher than 2, the theory of large g values, based on the spin Hamiltonian (Brodbeck, 1980)

$$\hat{H} = \beta \mathbf{SgB} + D(S_z^2 - S(S+1)/3) + E(S_x^2 - S_y^2)$$

was used for the interpretation of the EPR spectra. β is the Bohr magneton, **S** the effective spin, **g** a second rank tensor with the eigenvalues g_x, g_y, g_z. D $(=3B_2^0)$ is the axial and E $(=B_2^2)$ the orthorhombic component which describes the splitting of the Fe^{3+} Kramers doublets in the crystal field. The orthorhombic character of the field is expressed by the ratio $E/D = \lambda$ where a completely rhombic field is achieved if $E/D = \lambda = 0.33$. $E/D = 0$ implies a crystal field of axial symmetry. A single EPR signal with $g_x = g_y = g_z = 4.27$ $(=g_{eff})$ will be observed when $\lambda = 0.33$ and $h\nu/D < 1$ ($h\nu$ is the microwave energy).

Values for g_x, g_y, g_z as a function of λ were calculated by Gaite and Michoulier (1970). According to this calculation the g_{eff} values of 4.3 and 3.9 correspond to g_z and $g_{x,y}$, respectively, of a Fe^{3+} center with $\lambda = 0.28$. This means that the crystal field at the Fe^{3+} centers in cristobalite and tridymite is of strong orthorhombic character. The shift of $g_{eff} = 4.3$ and 3.9 towards higher and lower values, respectively, indicates a decrease of the orthorhombic character of the crystal field with increasing temperature.

Cristobalite

Grunin and Pavlova (1971) suggested that Fe^{3+} enters the cristobalite structure at interstitial sites. In contrast, microchemical studies on iron-bearing cristobalites from used silica refractory bricks suggested an incorporation of Fe^{3+} at the place of Si^{4+} if the Fe_2O_3 content of the silica phase is low ($\leq$0.05 wt.%), but a tetrahedral and interstitial incorporation if the Fe_2O_3 content is high ($\geq$0.05 wt.%). Charge balance was believed to be achieved by interstitial incorporation of alkali or alkaline-earth ions, and in the case of higher Fe_2O_3 content additionally by interstitial incorporation of Fe^{3+} (Schneider and Majdic, 1984). With respect to our samples, we believe that Fe^{3+} favorably enters the Si^{4+} positions. The low Fe^{3+} content incorporated into cristobalite supports this. Since the ionic radii of Si^{4+} (0.26 Å) and Fe^{3+} (0.49 Å, tetrahedral coordination, Shannon and Prewitt, 1969) differ considerably in size, Fe^{3+} for Si^{4+} substitution can be expected only if Fe content is low. The structure refinement of low cristobalite (Dollase, 1965) yielded one silicon and one oxygen position corresponding to a regular SiO_4 tetrahedron. If the Fe^{3+} to Si^{4+} substitution produced a regular FeO_4 complex, the EPR spectrum should exhibit a signal

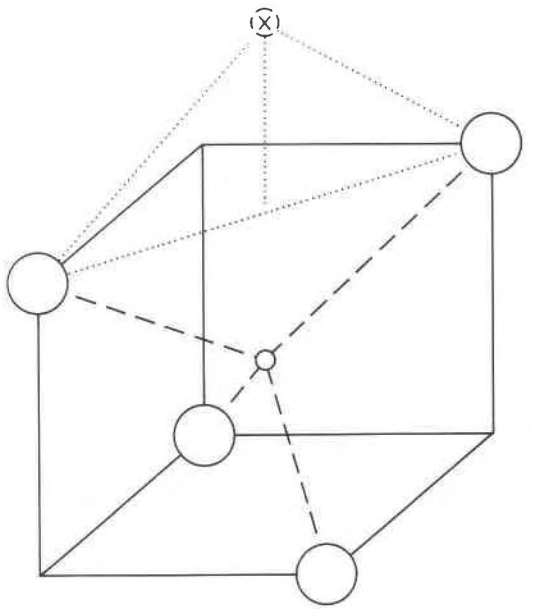

Fig. 4. The paramagnetic $Fe^{3+}O_4Na^+$ complex with C_{2v} symmetry (after Loveridge and Parke, 1971). ○ = Fe^{3+}; ○ = O; × = Na^+.

at $g_{eff} = 2$. This was not observed, but a signal group near 4.3 appeared instead. Loveridge and Parke (1971) pointed out that an EPR signal can be expected at $g_{eff} = 4.3$ if the tetrahedral paramagnetic complex has a MA_2B_2 configuration with C_{2v} symmetry. M corresponds to Fe^{3+} and A and B to structurally non-equivalent oxygens. Another possibility to build a complex with C_{2v} symmetry is to combine the tetrahedral iron-oxygen groups with adjacent Na^+ ions occurring in structural voids to a charge-balanced complex $Fe^{3+}O_4Na^+$ (Fig. 4). In order to satisfy the C_{2v} symmetry, the Na^+ ions must lie on the C_2 axis of the complex. Such complexes are possible in cristobalite, since Si^{4+} lies on a twofold axis which precisely points to the center of a neighboring void. However, on the basis of our EPR data we cannot decide whether the signals arise from a complex of the type $Fe^{3+}O_4Na^+$ or $Fe^{3+}O_2^AO_2^B$.

The split EPR lines at $g_{eff} = 4.33$ and 4.3, and the structure of the EPR line at $g_{eff} = 3.91$ (Fig. 1) suggest that two structurally inequivalent Fe^{3+} centers occur in cristobalite. The occurrence of two inequivalent cation sites has also been discussed for V^{4+}-substituted cristobalites (Grunin, 1971). Dollase's space group of low cristobalite, $P4_12_12$, allows only one cation position. This discrepancy may be explained as follows: the Fe^{3+} incorporation causes a symmetry lowering from $P4_12_12$ to $C222_1$ which is a subgroup of $P4_12_12$ and actually contains two cation positions in accordance with the two observed Fe^{3+} centers. On the other hand the finding of two slightly different Si-O distances, and of four different tetrahedral angles in cristobalite (Dollase, 1965) may suggest that the true symmetry of low cristobalite is lower than that published by Dollase, due to a non-regular tetrahedral site, and hence, contains

more than one cation site. Again, from the EPR data it cannot be decided whether the two Fe^{3+} centers can be explained by symmetry lowering which is due to a local deformation of the oxygen tetrahedra caused by Fe^{3+} to Si^{4+} substitution, or if in pure low cristobalite the tetrahedra are distorted due to factors inherent in the structure itself. However, the EPR data raise the question of the true symmetry of cristobalite.

The temperature-induced merging of the EPR signals around $g_{eff} = 4.3$ to one single peak above room temperature indicates that the two Fe^{3+} centers become structurally indiscernible with the increase of temperature. The low merging temperature shows that the difference between the two physically inequivalent Fe^{3+} centers is rather small. This means that the two cation sites differ only slightly with respect to their structural environment and that the crystal field at the two Fe^{3+} sites must be very similar.

Tridymite

The similarity of the EPR spectra of tridymite and cristobalite implies that the incorporation mode is comparable in the two phases. This is reasonable because of the close structural relationships between cristobalite and tridymite. The poor resolution of the tridymite EPR signals is explained by its distorted low-temperature structure (Kato and Nukui, 1976; Konnert and Appleman, 1978): Si_2O_7 groups of tridymite having their trigonal axis parallel to **c** display a strong expansion-induced distortion along **c**, which is caused by the unfavorable *cis*-configuration of oxygen atoms (see Schneider et al., 1979, fig. 6). On the other hand, all Si_2O_7 groups in cristobalite are in the stable *trans*-configuration. A possible conclusion is that a number of slightly different Fe^{3+} centers occurring in tridymite give rise to a couple of EPR signals, which lie so closely together that they cannot be resolved.

Glass sample

The shape of the EPR signal at $g_{eff} = 4.2$ of the glass sample is similar to the shape of the corresponding signals in cristobalite and tridymite. Therefore, a similar short-range order of the SiO_4 tetrahedra in glass as well as in cristobalite and tridymite can be assumed. A tridymite-like short-range order of silica glass has also been inferred from infrared spectroscopic studies (Lippincott et al., 1958; Hanna, 1965). The EPR signal at $g_{eff} = 2$ which only appears in the spectrum of the glass sample but not in those of cristobalite and tridymite shows a line shape which corresponds to a paramagnetic center with axial symmetry (Meads and Malden, 1974). Such signals are found in non-crystalline silicates and are attributed to oxygen-associated hole centers (Friebeck et al., 1976). Thus, the absence of the EPR signal at $g_{eff} = 2$ in the cristobalite and tridymite spectra may be taken as a criterion that the investigated samples were glass-free. The broad EPR signal at $g_{eff} = 8$ is explained by hematite submicroscopically dispersed in the glass sample.

Acknowledgments

The authors are grateful to Dr. D. E. Appleman for critical reading of the manuscript and valuable comments.

References

Brodbeck, C. M. (1980) Investigations of *g*-values correlations associated with the $g = 4.3$ ESR signal of Fe^{3+} in glass. Journal of Non-Crystalline Solids, 40, 305–313.

Busche, F. D., Conrad, G. H., Keil, K., Prinz, M., Bunch, T. E., Erlichman, J., and Quaide, W. L. (1971) Electron Microprobe Analyses of Minerals from Apollo 12 Lunar Samples. Department of Geology and Institute of Meteorites, The University of New Mexico, Special Publication Number 3.

Chesters, J. H. (1973) Refractory Production and Properties. The Steel and Iron Institute, London.

Dollase, W. A. (1965) Reinvestigation of the structure of low cristobalite. Zeitschrift für Kristallographie, 121, 369–377.

Friebeck, E. J., Griscom, D. L., and Siegel, G. H., Jr. (1976) Radiation induced defect centers in non-crystalline SiO_2. In G. H. Frischat, Ed., Non-Crystalline Solids. Trans Tech Publications, Switzerland.

Frondel, J. W. (1975) Lunar Mineralogy. John Wiley & Sons, New York.

Gaite, J. M. and Michoulier, J. (1970) Application de la résonance paramagnétique électronique de l'ion Fe^{3+} à l'étude de la structure des feldspaths. Bulletin de la Société française de Minéralogie et de Cristallographie, 93, 341–356.

Grunin, V. S. (1971) EPR of V^{4+} Ions in cristobalite. Soviet Physics Solid State, 12, 1785–1788.

Grunin, V. S. and Pavlova, G. A. (1971) EPR of Fe^{3+} ions in cristobalite and quartz glass. Soviet Physics Solid State, 13, 637–639.

Hanna, R. (1965) Infrared absorption spectrum of silicon dioxide. Journal of the American Ceramic Society, 48, 595–599.

Kato, K. and Nukui, A. (1976) Die Kristallstruktur des monoklinen Tief-Tridymits. Acta Crystallographica, B32, 2486–2491.

Konnert, J. H. and Appleman, D. E. (1978) The crystal structure of low tridymite. Acta Crystallographica, B34, 391–403.

Lippincott, E. R., Van Valkenburg, A., Weir, C. E., and Bunting, E. N. (1958) Infrared studies on polymorphs of silicon dioxide and germanium dioxide. Journal of Research of the National Bureau of Standards, 61, 61–70.

Loveridge, D. and Parke, S. (1971) Electron spin resonance of Fe^{3+}, Mn^{2+}, and Cr^{3+} in glasses. Physics and Chemistry of Glasses, 12, 19–27.

Mason, B. (1972) Lunar tridymite and cristobalite. American Mineralogist, 57, 1530–1535.

Mason, B. (1953) Tridymite and christensenite. American Mineralogist, 38, 866–867.

Meads, R. E. and Malden, P. J. (1974) Electron spin resonance in natural kaolinites containing Fe^{3+} and other transition metal ions. Clay Minerals, 10, 313–345.

Patzak, I. and Konopicky, K. (1962) Studien an Tridymiten. Berichte der Deutschen Keramischen Gesellschaft, 39, 168–174.

Schneider, H., Flörke, O. W., and Majdic, A. (1979) Thermal expansion of tridymite. Proceedings of the British Ceramic Society, 28, 267–279.

Schneider, H. and Majdic, A. (1984) Iron incorporation in tridymite and cristobalite. Neues Jahrbuch für Mineralogie, Monatshefte, 559–568.

Schneider, H., Wohlleben, K., and Majdic, A. (1980) Incorporation of impurities in tridymites from a used silica brick. Mineralogical Magazine, 43, 879–883.

Seifert-Kraus, U. and Schneider, H. (1984) Cation distribution between cristobalite, tridymite, and coexisting glass phase in used silica bricks. Ceramics International, 10, 135–142.

Shannon, R. D. and Prewitt, C. T. (1969) Effective ion radii in oxides and fluorides. Acta Crystallographica, B25, 925–946.
Smith, J. V. and Steele, J. M. (1984) Chemical substitution in silica polymorphs. Neues Jahrbuch für Mineralogie, Monatshefte, 137–144.
Wlotzka, F., Fredriksson, K., Palme, H., Spettel, B., Noonan, A. F., and Wänke, H. (1983) Alkali differentiation in LL-chondrites. Geochimica et Cosmochimica Acta, 47, 743–757.

Manuscript received, February 6, 1985;
accepted for publication, August 31, 1985.